# Silver Oxide Nanowalls Grown on Cu Substrate as an Enzymeless Glucose Sensor

**Bin Fang,* Aixia Gu, Guangfeng Wang, Wen Wang, Yuehua Feng, Cuihong Zhang, and Xiaojun Zhang***

College of Chemistry and Materials Science, Anhui Key Laboratory of Functional Molecular Solids, and Anhui Key Laboratory of Chem-Biosensing, Anhui Normal University, Wuhu 241000, P R China

**ABSTRACT** $Ag_2O$ nanowalls consisting of densely packed nanoplates based on a Cu substrate were synthesized through a facile one-pot hydrothermal method. A new enzymeless glucose sensor of Cu−$Ag_2O$ nanowalls was fabricated. The Cu−$Ag_2O$ nanowalls showed higher catalysis on glucose oxidation than traditional $Ag_2O$ nanoflowers and Cu−$Ag_2O$ nanospindles. At an applied potential of 0.4 V, the sensor produced an ultrahigh sensitivity to glucose (GO) of 298.2 $\mu$A $mM^{-1}$. Linear response was obtained over a concentration range from 0.2 mM to 3.2 mM with a detection limit of 0.01 mM (S/N = 3). Satisfyingly, the Cu−$Ag_2O$ nanowalls modified electrode was not only successfully employed to eliminate the interferences from uric acid (UA) acid ascorbic (AA) and also fructose (FO) during the catalytic oxidation of glucose. The Cu−$Ag_2O$ nanowalls modified electrode allows highly sensitive, excellently selective, stable, and fast amperometric sensing of glucose and thus is promising for the future development of nonenzymatic glucose sensors.

**KEYWORDS:** $Ag_2O$ nanowalls • glucose sensor • electocatalysis • enzymeless

## INTRODUCTION

For both clinical biochemistry and food industry, knowledge of glucose (GO) concentration within a sample is so important that much work has gone into developing effective methods for its measurement (1). Amperometric glucose biosensors are one such promising methodology. Most previous studies on this subject involves the use of enzyme glucose oxidase (GODx) (2, 3), which catalyzes the oxidation of glucose to gluconolactone. This method provides great selectivity but the sensors are limited by the sensitivity of the enzyme to temperature, pH value, humidity, and toxic chemicals (4). All those are why enzymeless glucose sensors receive keen interests. Early research has focused on the use of noble metal-based, including Pt (5, 6), Au (7, 8), and so on, and alloy-based (containing Pt, Ru, Pb, Au, and Cu) amperometric glucose sensors (7−10). However, these electrodes often have drawbacks of low sensitivity and poor stability caused by surface poisoning from the adsorbed intermediates (9) and chloride (10). In recent years, nanomaterials with special physical and chemical properties have been widely applied in chemsensors and biosensors. Therefore, it is an important strategy in the construction of enzymeless glucose sensors with nanomaterials. Ye et al. reported that carbon nanotube with high electrical conductivity was utilized to construct enzymeless glucose biosensors (11), Yu et al. applied Pt nanoparticles supported on carbon nanotubes to fabricate nonenzymatic glucose biosensors (12), Zhu et al. prepared DMG functionalized copper nanoparticles to construct an enzyme-free glucose biosensor (13), Bai and his co-workers developed an enzyme-free glucose sensor using a three-dimensional inverse-opal gold film (14). However, the functionalizing procedures are usually complicated, time-consuming and expensive. Furthermore, the research conducted in this area has been concentrated on nanoparticles and carbon nanotubes based materials, there is no report about sensors based $Ag_2O$ to determine glucose.

Fructose (FO), which is isomeric with glucose, usually coexists with glucose in many biologic and food samples (15), and thus it is difficult to detect glucose when fructose is present. It is well-known that spectrophotometry is a good method for differentiating glucose from fructose in samples (16, 17). However, the method is time-consuming and requires complex pretreatment. Hence, developing a time-saving and facile method is awfully important and necessary. Recently, amperometric method has been widely used in biological and food analysis for its facility, sensitivity and accuracy. As we know, there are few reports on distinguishing glucose from fructose by amperometric methods (18, 19); nevertheless, they are complicated, high cost, and difficult to apply. Hence, construction of a new sensor to facilitate glucose detection when fructose is present should be demonstrated.

In this paper, we present the fabrication of an enzymeless amperometric sensor based on Cu−$Ag_2O$ nanowalls for effective detection of glucose for the first time. The Cu−$Ag_2O$ nanowalls exhibited higher catalytic effect on glucose oxidation than traditional $Ag_2O$ nanoflowers and Cu−$Ag_2O$ nanospindles. Exhilaratingly, interferences from UA, AA, and even fructose were effectively avoided at the Cu−$Ag_2O$ nanowalls modified electrode.

* Corresponding author. E-mail: binfang_47@yahoo.com.cn, zhangxiaojun173@yahoo.com.cn.
Received for review August 26, 2009 and accepted November 13, 2009

DOI: 10.1021/am900576z

## EXPERIMENTAL SECTION

**Chemicals.** $AgNO_3$, $NH_3 \cdot H_2O$, $H_2O_2$, and Cu substrate were purchased from Shanghai Chemical Corp. Glucose and fructose were purchased from Sigma. All chemicals were used as received without any further purification. Millipore water was used in all experiments.

**Synthetic Procedures.** A clean Cu substrate (1.5 cm × 1.5 cm × 0.25 cm) was prepared from a consecutive ultrasonication in acetone, ethanol, and distilled water. In a typical procedure, the prepared Cu substrate was immersed in a 60 mL steel autoclave containing 4 mL $NH_3 \cdot H_2O$ (1 M) and 20 mL $AgNO_3$ (0.1 M) solution stirred vigorously to homogeneity. The steel autoclave was sealed, maintained at 100 °C for 8 h (for Cu−$Ag_2O$ nanospindles, the steel autoclave was maintained at 100 °C for 4 h), and then cooled naturally to room temperature. The black precipitate scraped from the Cu substrate was washed with ethanol and distilled water for several times before characterizations. The $Ag_2O$ nanoflowers were synthesized under the same conditions without Cu substrate. The Cu nanoparticles were produced according to the literature (20).

**Apparatus.** X-ray powder diffraction (XRD) patterns of the products were recorded on a Shimadzu XRD-6000 employing a scanning rate of 0.05° $s^{-1}$ with the $2\theta$ range from 30 to 80°, with high-intensity Cu K$\alpha$ radiation ($\lambda = 0.154178$ nm). X-ray photoelectron spectroscopy (XPS) data were acquired on a Thermo ESCALAB 250 X-ray photoelectron spectrometer with an Al K$\alpha$ excitation source (1486.6 eV). Filed-emission scanning electron microscopes (FESEM) images were obtained using Hitachi S-4800 SEM (operated at 10 kV). Electrochemical impedance spectroscopy (EIS), cyclic voltammetry (CV) and amperometric experiments were performed on a model CHI 660B electrochemical analyzer (ChenHua Instruments Co. Ltd., Shanghai, China) coupled to a computer.

**Construction of the Modified Electrodes.** Glass carbon electrode (GCE) (3 mm diameter) was cleaned according to the literature (21). The fabrication of Cu−$Ag_2O$ nanowalls modified electrode is described as follows: 10 mg of Cu−$Ag_2O$ nanowalls was dissolved into 1 mL of distilled water. Approximate 15 min of ultrasonication was necessary to obtain homogeneously dispersed Cu−$Ag_2O$ nanowalls. After dropping 10 $\mu$L of the mixture onto the prepared electrode surface, the electrode was dried at room temperature. Finally, 5 $\mu$L of Nafion was cast onto the surface and allowed to dry for 24 h to form a uniform structure. The same process was applied to prepare the $Ag_2O$ nanoflowers modified electrode, Cu−$Ag_2O$ nanospindles modified electrode and Cu nanoparticles modified electrode, the resulting electrodes were named Cu−$Ag_2O$ NWS/GCE, $Ag_2O$ NFs/GCE, Cu−$Ag_2O$ NDS/GCE, and Cu NPS /GCE, respectively. For EIS, Nafion was unwanted.

**Electrochemical Experiments.** All electrochemical experiments were conducted using a three-electrode electrochemical cell with a working electrode (Cu−$Ag_2O$ NWS/GCE, $Ag_2O$ NFS/GCE, Cu−$Ag_2O$ NDS/GCE or Cu NPS/GCE), an Ag/AgCl reference electrode and a platinum wire auxiliary electrode, respectively. All potentials in this paper are referenced to the Ag/AgCl. EIS was obtained at different electrodes in 0.1 M KCl containing 5 mM $K_3[Fe(CN)_6]/K_4[Fe(CN)_6]$ (1:1). For CV and amperometric experiment, $N_2$ was allowed to deaerate for 10 min and to flow over the solution during the whole experiment to avoid any interference coming from $O_2$. Electrochemical catalytic behaviors of different electrodes toward glucose oxidation were characterized by CV in 0.1 M NaOH at a scan rate of 50 mV $s^{-1}$. The Cu−$Ag_2O$ NWS/GCE was evaluated as a glucose sensor in 0.1 M NaOH at a desired potential and the amperometric curves were obtained after adding a certain concentration of glucose with the solution stirred constantly.

## RESULTS AND DISCUSSION

The identity and crystal structure of the $Ag_2O$ nanowalls were first verified by XRD analysis. Figure 1A gives XRD patterns of the sample. All the major diffraction peaks located at (111), (200), (220), and (311) can be indexed to the monoclinic $Ag_2O$ phase with lattice constants according to the reported date (JCPDS Card 75−1532). The component of our materials was further characterized by XPS technique, as indicated in Figure 1B−E. The curve in Figure 1E is the typical peak of $Cu2p_{3/2}$ and $Cu2p_{1/2}$, from which one can see that existence of Cu (0) in the morphology is major, whereas minor existence of Cu (II) may be attributed to the surface oxidation of the products. Figure 2a−d shows FESEM images of different nanomaterials. Figure 2a is typical FESEM image of $Ag_2O$ nanowalls arranged on the Cu substrate. The image of Cu−$Ag_2O$ nanowalls displays that a large amount of $Ag_2O$ nanocrystals self-organize into wall-like blocks. Most of the $Ag_2O$ nanocrystals with uniform morphology are upright and outward, densely packed, and well-aligned, composing nanowalls (Figure 2b). Wall-like structures are made up of nanoplatelets with the thickness of 20−30 nm, width of 200−400 nm, and length of 100−400 nm. For further study, we provided the SEM images of $Ag_2O$ nanoflowers and Cu−$Ag_2O$ nanospindles (Figure 2c, d). The $Ag_2O$ nanoflowers are also assembled from nanoplates but the nanoplates are thinly packed (Figure 2c). One can see that a large amount of nanospindles are arrayed on the Cu substrate (Figure 2d).

EIS was applied to monitor the whole procedure in preparing modified electrodes, which could provide useful information for each step and be used for probing the changes of the surface modification (22). One can see in Figure 3 that the bare GCE exhibits an almost straight line, which is characteristic of a diffusion limited electrochemical process (curve a). After Cu−$Ag_2O$ nanowalls, $Ag_2O$ nanoflowers, and Cu−$Ag_2O$ nanospindles being cast on the bare GCE, the semicircle diameter of EIS, $R_{et}$, increases as compared with that at the bare GCE. The impedance changes show that $Ag_2O$ nanomaterials are attached to the electrode surface. Whereas, $R_{et}$ is different when different $Ag_2O$ nanomaterials are cast onto the bare GCE. As Figure 3 shows, $R_{et}$ is $Ag_2O$ NFS/GCE (curve d) > Cu−$Ag_2O$ NDS/GCE (curve c) > Cu−$Ag_2O$ NWS/GCE (curve b), predicating the electron transfer ability is Cu−$Ag_2O$ nanowalls > Cu−$Ag_2O$ nanospindles > $Ag_2O$ nanoflowers.

Figure 4A−D shows CV images for different electrodes in absence and presence of 0.1 mM glucose. There is no response for glucose oxidation at the bare GCE, as can be seen from curves 9 and 10 of Figure 4A. However, a pair of well-defined redox peaks at the Cu−$Ag_2O$ NWS/GCE is obtained. As Figure 4A shows, the peak current increases obviously after glucose being added to the 0.1 M NaOH (curves 1, 2).

We also compared the electrochemical response of glucose oxidation at the Cu−$Ag_2O$ NWS/GCE with that at $Ag_2O$ NFS/GCE, Cu−$Ag_2O$ NDS/GCE and Cu NPS/GCE (Figure 4B, C and D). As curves 3 and 4 of Figure 4B show, although $Ag_2O$ NFS/GCE has an improved effect on the glucose oxidation, the larger increment of the peak current and more

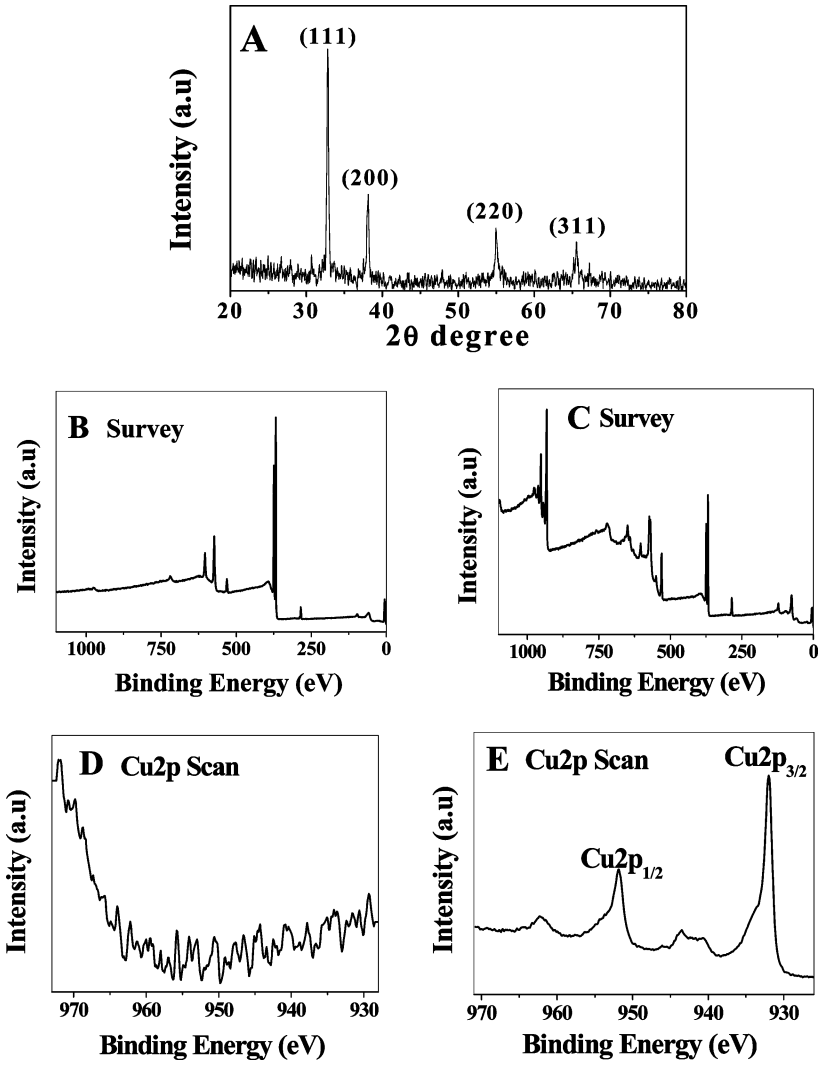


**FIGURE 1. (A) XRD pattern of the as-synthesized Cu−$Ag_2O$ nanowalls; (B−D) XPS analysis of $Ag_2O$ nanoflowers (B, D) and Cu−$Ag_2O$ nanowalls (C, E).**

well-defined peak appear at the Cu−$Ag_2O$ NWS/GCE, which displays the response at Cu−$Ag_2O$ NWS/GCE is better. And the instance is same with Cu−$Ag_2O$ NDS/GCE ((Figure 4C). However, the peak current hardly changes at the Cu NPS/GCE for absence and presence of glucose (curves 7, 8 of Figure 4D) compared with the CV curves of the Cu−$Ag_2O$ NWS/GCE (curves 1, 2 of Figure 4D). One can conclude that the redox waves observed at the Cu−$Ag_2O$ NWS/GCE are attributed only to $Ag_2O$.

As the above phenomena show, the Cu−$Ag_2O$ nanowalls have higher catalysis on glucose oxidation than other two nanostuctures (Cu−$Ag_2O$ nanospindles, $Ag_2O$ nanoflowers). This may be a direct result of the special structure of the Cu−$Ag_2O$ nanowall. As we know, the aspect ratio of the densely packed Cu−$Ag_2O$ nanowalls is larger than that of the Cu−$Ag_2O$ nanospindles, which results in Cu−$Ag_2O$ nanowalls promoting electron transfer better. To attest it, we measured the electrochemical active surface (EAS) of the two electrodes at 30 °C in 0.1 M NaOH by CV. According to ref 23, the peaks in the potential region $-800$ mV $< E <$ $-500$ mV on the CV curve are associated with the hydrogen adsorption process in the anodic scan. The EAS is calculated according to eq 1 (24)

$$\mathrm{EAS} = 4.76Q_{\mathrm{H}}/[\mathrm{MO}] \qquad (1)$$

where $Q_{\mathrm{H}}$ denotes the Coulombic charge for hydrogen desorption at the electrodes (mC $cm^{-2}$) and [MO] represents the nanomaterials (Cu−$Ag_2O$ nanowalls or Cu−$Ag_2O$ nanospindles) loading (mg $cm^{-2}$) on the electrode. The EAS for Cu−$Ag_2O$ nanowalls/GCE is 25.53 $m^2$ $g^{-1}$ and for Cu−$Ag_2O$ nanospindles/GCE is 1.55 $m^2$ $g^{-1}$. The results indicate that the EAS for Cu−$Ag_2O$ nanowalls is much larger than that of Cu−$Ag_2O$ nanospindles, which is consonant with our estimation. Furthermore, the electric Cu in the center of the Cu−$Ag_2O$ nanowalls provides more electron transfer passages than $Ag_2O$ nanoflowers, so the electrochemical probe could arrive to the surface of the electrode more easily (25).

The amperometric response of the Cu−$Ag_2O$ NWS/GCE upon successive addition of glucose to 0.1 M NaOH at an applied potential of 0.4 V is shown in Figure 5A. A subsequent addition of glucose to NaOH solution with stirring produces a remarkable increase in the current. The response time is <5 s, revealing the faster response of the sensor than that of previously reported glucose sensors (12, 13, 26−29).

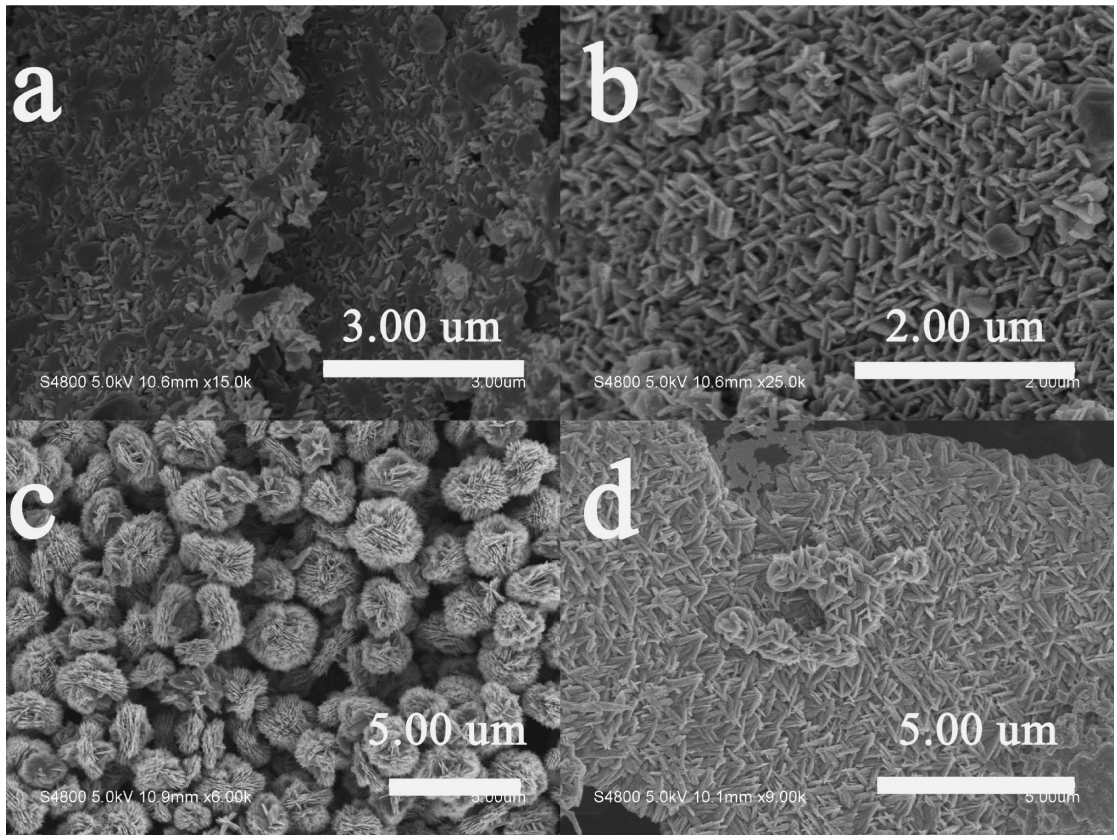


**FIGURE 2. (a) Typical FESEM image of the $Ag_2O$ nanowalls on Cu substrate; (b) FESEM image of the $Ag_2O$ nanowalls; (c) FESEM image of the $Ag_2O$ nanoflowers; (d) FESEM image of the Cu−$Ag_2O$ nanospindles.**

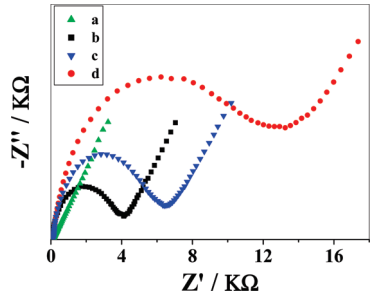


**FIGURE 3. EIS obtained at (a) a bare GCE, (b) Cu−$Ag_2O$ NWS/GCE, (c) Cu−$Ag_2O$ NDS, and (d) $Ag_2O$ NFS/GCE in 0.1 M KCl containing 5 mM $K_3[Fe(CN)_6]/K_4[Fe(CN)_6]$ (1: 1).**

The calibration plot of the sensor under the optimized experimental conditions is shown in Figure 5B. The calibration range of glucose is done from 0.2 to 3.2 mM. The linear response corresponds to an ultrahigh of 298.2 $\mu$A $mM^{-1}$, which can be seen that the Cu−$Ag_2O$ NWS/GCE is far more sensitive toward the detection of glucose compared with other sensors (26−28, 30). And the detection limit is estimated, based on signal-to-noise ratio (S/N) of 3, to be 0.01 mM.

One of the most important analytical factors for an amperometric biosensor is the selectivity of the sensor to target analyte. It is well-known that uric acid (UA) and ascorbic acid (AA) are common interfering species during catalytic oxidation of glucose. Thus, we conducted the interference test by measuring currents changes caused by addition of UA and AA during glucose sensing. Amperometric response was obtained by successive injection of 4 mM glucose and interfering species (4 mM UA and 4 mM AA). As shown in Figure 6A, the response of the Cu−$Ag_2O$ NWs/GCE to 4 mM glucose is not affected by addition of 4 mM UA and AA, respectively. The normal physiological level of glucose (3−8 mM) is much higher than those of UA (0.1 mM), AA (0.1 mM). Therefore, the present electrode can successfully avoid interferences from UA and AA. Furthermore, we performed the interference test to demonstrate the ability of the sensor to differentiate glucose from fructose, which is isomeric with glucose. We can see that influence from fructose could be neglected until the concentration comes up to 0.5 mM, which is five times that of glucose (the current response for the fructose oxidation is 5% of that of glucose), indicating excellent selectivity of the sensor toward glucose detection (Figure 6B).

In order to demonstrate the applicability of the proposed biosensor to mock sample analysis, 0.5, 1.0, and 2.0 mM glucose solution were prepared, respectively. The results obtained as mean from five determinations are shown in Table 1. The results are satisfying.

The stability of the Cu−$Ag_2O$ NWS/GCE was examined by monitoring the remaining amount of current response after successively cycling the modified electrode for 200 circles. It is found that the peak current for glucose oxidation retains 96% of its initial value and no obvious potential shift is observed. The biosensor was stored at room temperature and its long-term stability was tested for 30 days. The activity of the electrode remains about 97% of its initial current response in the first 10 days and gradually decreases after

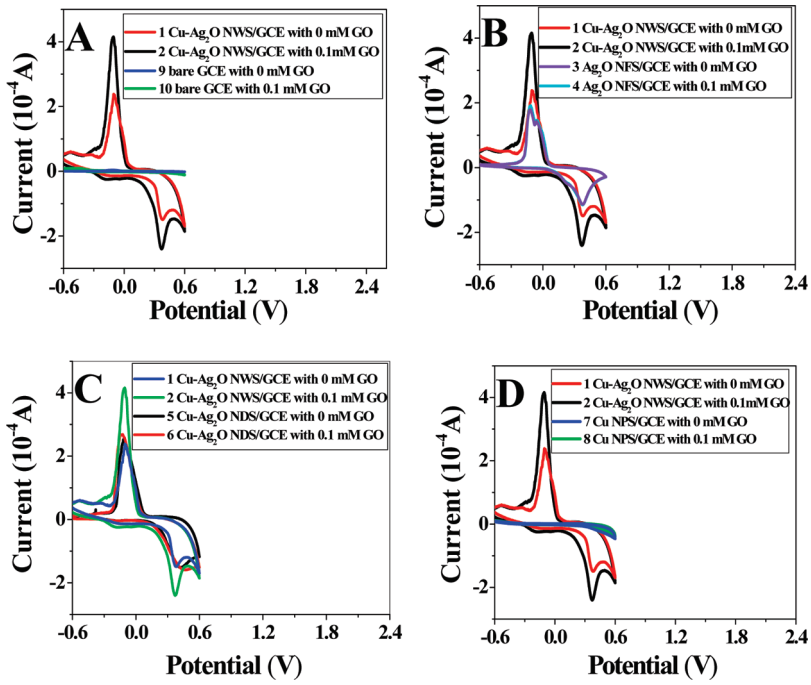


FIGURE 4. (A−D) CV images for different electrodes in the absence (curves 1, 3, 5, 7, and 9) and presence (curves 2, 4, 6, 8, and 10) of 0.1 Mm glucose in 0.1 M NaOH at a scan rate of 50 mV $s^{-1}$: curves 1, 2 for Cu−$Ag_2O$ NWS/GCE, curves 3, 4 for $Ag_2O$ NFS/GCE, curves 5, 6 for Cu−$Ag_2O$ NDS/GCE, curves 7, 8 for Cu NPS/GCE, curves 9, 10 for bare GCE, respectively.

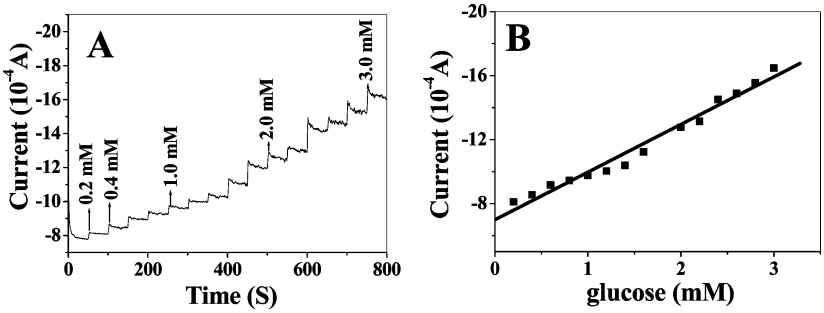


FIGURE 5. (A) Typical amperometric response of Cu−$Ag_2O$ NWS/GCE to successive injection of glucose into 0.1 M NaOH with stirring, the working potential was 0.4 V. (B) Calibration curve and linear plot of response current vs glucose concentration.

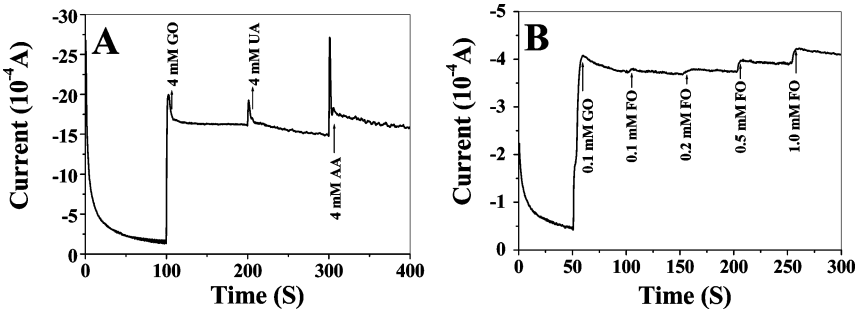


FIGURE 6. (A) Amperometric response for successive injection of 4 mM GO and interfering species (4 mM UA and 4 mM AA) into 0.1 M NaOH with stirring, the working potential was 0.4 V. (B) Successive injection of GO (0.1 mM) and FO (0.1, 0.2, 0.5, and 1.0 mM) into 0.1 M NaOH with stirring, the working potential was 0.4 V.

20 days. The biosensor holds 90 % of the initial performance even after 30 days. The high stability of the modified electrode can be related to the Cu substrate, which increases the effective surface area and stabilizes the activity of $Ag_2O$ nanostructure. To test the repeatability of the sensor, we performed 7 successive measurements at a glucose concentration of 0.1 mM. It was found that the relative standard

**Table 1. Results for the Determination of Glucose in Artificial Solution**

| sample | content (mM) | found (mM) | RSD (%) ($n = 5$) | recovery (%) |
|---|---|---|---|---|
| 1 | 0.5 | 0.52 | 1.2 | 104 |
| 2 | 1.0 | 0.98 | 1.5 | 98 |
| 3 | 2.0 | 2.01 | 1.35 | 100.5 |

deviation (R.S.D.) was 2.7%, indicating an acceptable reproducibility.

## CONCLUSIONS

In summary, we have synthesized $Ag_2O$ nanowalls made up of densely packed nanoplates based on a Cu substrate. The nanowalls were incorporated, along with nafion, into an enzymeless glucose sensor which displayed a good performance. Compared with $Ag_2O$ NFS/GCE, Cu−$Ag_2O$ NDS/GCE and Cu NPS/GCE, the Cu−$Ag_2O$ NWS/GCE displays higher catalytic activity toward the glucose oxidation. It shows a significant linear dependence ($R = 0.998$) in the glucose concentration up to 3.2 mM. Satisfyingly, the Cu−$Ag_2O$ NWS/GCE could not only effectively avoid the interferences from the common interfering species such UA and AA but also fructose, an isomer of glucose. High sensitivity, excellent selectivity, good stability and repeatability give it potential for the future development of nonenzymatic glucose sensors.

**Acknowledgment.** This work was supported by the National Natural Science Foundation of China (20675001, 20901003), Anhui Key Laboratory of Controllable Chemistry Reaction & Material Chemical Engineering, the Young Teacher Program of Anhui Normal University (2009xqnzc19), and the Natural Science Foundation of Educational Department of Anhui Province (KJ2008B167, No. KJ2009B013Z).

### REFERENCES AND NOTES

(1) Wilson, G. S.; Gifford, R. *Biosens. Bioelectron.* **2005**, *20*, 2388–2403.
(2) Kang, X. H.; Mai, Z. B.; Zou, X. Y.; Cai, P. X.; Mo, J. Y. *Anal. Biochem.* **2007**, *369*, 71–79.
(3) Zou, Y. J.; Xiang, C. L.; Sun, L. X.; Xu, F. *Biosens. Bioelectron.* **2008**, *23*, 1010–1016.
(4) Wilson, R.; Turner, A. P. F. *Biosens. Bioelectron.* **1992**, *7*, 165–185.
(5) Beden, B.; Largeaud, F.; Kokoh, K. B.; Lamy, C. *Electrochim. Acta* **1996**, *41*, 701–709.
(6) Kang, X. H.; Mai, Z. B.; Zou, X. Y.; Cai, P. X.; Mo, J. Y. *Talanta* **2008**, *74*, 879–886.
(7) Tominaga, M.; Shimazoe, T.; Nagashima, M.; Kusuda, H.; Kubo, A. *J. Electroanal. Chem.* **2006**, *590*, 37–46.
(8) Qiu, R.; Zhang, X. L.; Qiao, R.; Li, Y.; Kim, Y. I.; Kang, Y. S. *Chem. Mater.* **2007**, *19*, 4174–4180.
(9) Sun, Y. P.; Buck, H.; Mallouk, T. E. *Anal. Chem.* **2001**, *73*, 1599–1604.
(10) Wang, J. P.; Thomas, D. F.; Chen, A. C. *Anal. Chem.* **2008**, *80*, 997–1004.
(11) Deo, R. P.; Wang, J. *Electrochem. Commun.* **2004**, *6*, 284–287.
(12) Rong, L. Q.; Yang, Ch.; Qian, Q. Y.; Xia, X. H. *Talanta* **2007**, *72*, 819–824.
(13) Xu, Q.; Zhao, Y.; Xu, J. Z.; Zhu, J. J. *Sens. Actuators, B* **2006**, *114*, 379–386.
(14) Bai, Y.; Yang, W. W.; Sun, Y.; Sun, C. Q. *Sens. Actuators, B* **2008**, *134*, 471–476.
(15) Surareungchai, W.; Deepunya, W.; Tasakorn, P. *Anal. Chim. Acta* **2001**, *448*, 215–220.
(16) Lee, S. J.; Saleemuddin, M.; Scheper, T.; Loos, H.; Sahm, H. J. *Biotechnology* **1994**, *36*, 39–44.
(17) Evmiridis, N. P.; Thanasoulias, N. K.; Vlessidis, A. G. *Anal. Chim. Acta* **1999**, *398*, 191–203.
(18) Campuzano, S.; Loaiza, O. A.; Pedrero, M.; Villena, F. J. M.; Pingarro, J. M. *Bioelectrochemistry* **2004**, *63*, 199–206.
(19) Antiochia, R.; Palleschi, G. *Anal. Lett.* **1997**, *30*, 683–697.
(20) Yao, W. T.; Yu, S. H.; Zhou, Y.; Jiang, J.; Wu, Q. S.; Zhang, L.; Jiang, J. *J. Phys. Chem. B.* **2005**, *109*, 14011–14016.
(21) Zhang, X. J.; Wang, G. F.; Zhang, W.; Hu, N. J.; Wu, H. Q.; Fang, B. *J. Phys. Chem.C* **2008**, *112*, 8856–8862.
(22) Feng, J. J.; Xu, J. J.; Chen, H. Y. *J. Electroanal. Chem.* **2005**, *585*, 44–50.
(23) Eileen, H. Y.; Scott, K.; Reeve, R. W. *J. Electroanal. Chem.* **2003**, *547*, 17–24.
(24) Xu, C. W.; Shen, P. K. *Chem. Commun.* **2004**, 2238–2239.
(25) Zhang, X. J.; Wang, G. F.; Liu, X. W.; Wu, J. J.; Li, M.; Gu, J.; Liu, H.; Fang, B. *J. Phys.Chem.C.* **2008**, *112*, 16845–16849.
(26) Chen, J.; Zhang, W. D.; Ye, J. S. *Electrochem. Commun.* **2008**, *10*, 1268–1271.
(27) Ye, J. S.; Wen, Y.; Zhang, W. D.; Gan, L. M.; Xu, G. Q.; Sheu, F. S. *Electrochem. Commun.* **2004**, *6*, 66–70.
(28) Özcan, L.; Sahin, Y.; Türk, H. *Biosens. Bioelectron.* **2008**, *24*, 512–517.
(29) Bai, Y.; Sun, Y. Y.; Sun, C. Q. *Biosens. Bioelectron.* **2008**, *24*, 579–585.
(30) Liu, Y.; Teng, H.; Hou, H. Q.; You, T. Y. *Biosens. Bioelectron.* **2009**, *24*, 3329–3334.

AM900576Z